Soluble TNFRp75 regulates host protective immunity against *Mycobacterium tuberculosis*

Roanne Keeton,[1] Nasiema Allie,[1] Ivy Dambuza,[1] Brian Abel,[1,2] Nai-Jen Hsu,[1] Boipelo Sebesho,[1] Philippa Randall,[1] Patricia Burger,[1] Elizabeth Fick,[1] Valerie F.J. Quesniaux,[3] Bernhard Ryffel,[3] and Muazzam Jacobs[1,4]

[1]Division of Immunology, Department of Clinical Laboratory Sciences and Institute of Infectious Disease and Molecular Medicine, University of Cape Town, Cape Town, South Africa. [2]Singapore Immunology Network, Agency for Science, Technology and Research, Singapore. [3]University of Orleans and CNRS UMR7355, Experimental and Molecular Immunology and Neurogenetics, Orleans, France. [4]National Health Laboratory Service, Johannesburg, South Africa.

Development of host protective immunity against *Mycobacterium tuberculosis* infection is critically dependent on the inflammatory cytokine TNF. TNF signals through 2 receptors, TNFRp55 and TNFRp75; however, the role of TNFRp75-dependent signaling in immune regulation is poorly defined. Here we found that mice lacking TNFRp75 exhibit greater control of *M. tuberculosis* infection compared with WT mice. TNFRp75$^{-/-}$ mice developed effective bactericidal granulomas and demonstrated increased pulmonary recruitment of activated DCs. Moreover, IL-12p40–dependent migration of DCs to lung draining LNs of infected TNFRp75$^{-/-}$ mice was substantially higher than that observed in WT *M. tuberculosis*–infected animals and was associated with enhanced frequencies of activated *M. tuberculosis*–specific IFN-γ–expressing CD4^{+} T cells. In WT mice, TNFRp75 shedding correlated with markedly reduced bioactive TNF levels and IL-12p40 expression. Neutralization of TNFRp75 in *M. tuberculosis*–infected WT BM-derived DCs (BMDCs) increased production of bioactive TNF and IL-12p40 to a level equivalent to that produced by TNFRp75$^{-/-}$ BMDCs. Addition of exogenous TNFRp75 to TNFRp75$^{-/-}$ BMDCs infected with *M. tuberculosis* decreased IL-12p40 synthesis, demonstrating that TNFRp75 shedding regulates DC activation. These data indicate that TNFRp75 shedding downmodulates protective immune function and reduces host resistance and survival; therefore, targeting TNFRp75 may be beneficial for improving disease outcome.

Introduction

Mycobacterium tuberculosis is a highly efficient intracellular pathogen that requires specific cellular adaptive Th1 immune responses for host protection. Successful control of *M. tuberculosis* relies not only on a complex but organized series of interactions among mycobacteria, antigen-presenting cells, and lymphocytes, but also on the coordinated production of chemokines and cytokines. Although redundancy has been illustrated for many cytokines, others such as TNF, IL-1, IL-12, and IFN-γ cannot be functionally replaced, and the absence of any of these proves lethal during *M. tuberculosis* challenge.

TNF and its corresponding receptors (TNFRs), TNFRp55 and TNFRp75 (encoded by *TNFRSF1A* and *TNFRSF1B*, respectively), are members of supergene families (1). TNF-mediated signaling has a significant influence on the outcome of several infectious diseases and contributes to protective immunity against fungal, viral, protozoan, and bacterial pathogens (2). TNF is synthesized as a membrane-bound protein that is cleaved to a soluble form by TNF converting enzyme (TACE) (3). Both forms of the ligand are bioactive and can signal as homotrimers through either of the receptors, although membrane-bound TNF is thought to preferentially signal through TNFRp75, and soluble TNF is partisan to TNFRp55 (4). TNFRp55 and TNFRp75 show structural similarity with respect to 4 cysteine-rich motifs found in their extracellular regions, but lack structural compatibility in their cytoplasmic domains (1, 4); consequently, post-binding events and cellular responses are different for each TNFR (5). Moreover, both TNFRp55 and TNFRp75 can be maintained either as a membrane-bound form or can be shed from the cell surface. The effect of shedding and its impact on bioactive ligand availability is controversial. Evidence proposing an antagonistic effect, where ligand signaling is inhibited, has been published (6, 7). Conversely, it was suggested that ligand interaction with soluble receptor may act agonistically, by enhancing the half-life of the ligand and hence increasing its bioavailability (8).

TNF deficiency has profound effects on protective immunity against *M. tuberculosis* (9–13), even though the homolog, lymphotoxin α (LTα), is able to signal through the same receptors (2). The role of TNF in protective immunity against mycobacterial infection has been extensively investigated using mice deficient for TNF signaling (9, 10, 13, 14) or by neutralization studies (11, 12). The more recent generation of mouse strains expressing only the membrane form of TNF has allowed for the investigation of the respective roles of soluble and membrane-bound TNF in host immune function during mycobacterial challenge (15–23).

TNF is important for the cell recruitment required in order to form granulomas that restrict bacilli replication and prevent bacterial dissemination (13, 24–26). The establishment and continued maintenance of the structural integrity of granulomas are key for host protection, as illustrated in gene-targeted mice that are defective for granuloma formation. Such animals are unable to control bacilli replication, resulting in bacterial dissemination and premature death after infection with either virulent or avirulent mycobacterial species (9–11, 13, 27). Nonetheless, excessive TNF has deleterious effects and is considered to significantly influence degradation of lung tissue through promoting severe inflammation (14, 28) and to aid in bacterial replication in alveolar macrophages (29).

Conflict of interest: The authors have declared that no conflict of interest exists.
Citation for this article: *J Clin Invest.* 2014;124(4):1537–1551. doi:10.1172/JCI45005.

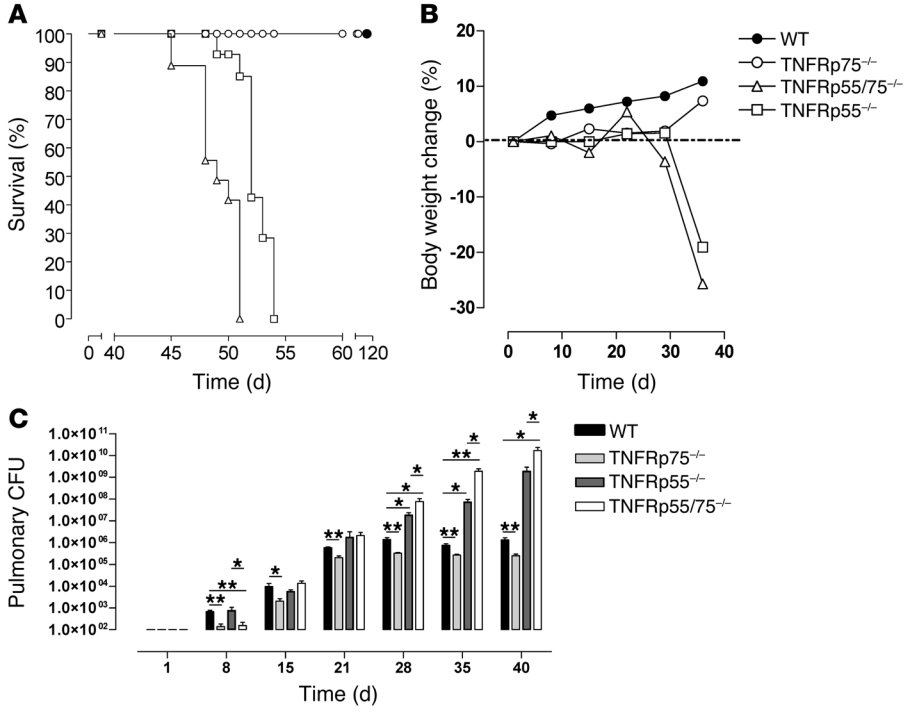

Figure 1
Enhanced acute control of *M. tuberculosis* replication in TNFRp75$^{-/-}$ mice. WT, TNFRp75$^{-/-}$, TNFRp55$^{-/-}$, and TNFRp55/75$^{-/-}$ mice were infected with 50–100 CFU *M. tuberculosis*. Mice were monitored for survival (**A**), and body weight changes were measured (**B**) (n = 10 per group). Pulmonary bacilli burden (**C**) was determined at the indicated time points by colony enumeration assay. Data (mean ± SEM of the CFU of 4 mice per time point) are representative of 3 similar experiments. *P < 0.05, **P < 0.01, ANOVA.

The role of TNFRp55 signaling in the host protective immune response to mycobacterial infections has been addressed in various mycobacterial infection models, including intravenous *M. tuberculosis* infection (24) and intraperitoneal *M. bovis* bacillus Calmette-Guerin (BCG) infection (26), in which TNFRp55 deficiency results in premature death. Mortality of TNFRp55-deficient mice during intravenous *M. avium* challenge was characterized by excessive T cell infiltration and was associated with IL-12–dependent disintegration of granulomatous lesions (30). Similar to TNF-deficient mice, TNFRp55-deficient mice displayed defective granuloma formation in response to *M. bovis* BCG infection, and treatment with anti-TNF mAb resulted in the regression of fully established granulomas in both TNF- and TNFRp55-deficient mice (11, 26). The similarity in phenotype between TNF- and TNFRp55-deficient mice suggests that TNFRp55 signaling is the major conduit for TNF-mediated immune function against mycobacterial infections. The role of TNFRp75 in host immune function during pathogen challenge, however, is controversial. Previous studies reported a protective role for TNFRp75 against *Histoplasma capsulatum* infection, in which TNFRp75 deficiency resulted in reduced IFN-γ production and premature mortality (31). In contrast, TNFRp75 was redundant for protection against *Listeria monocytogenes*, while it had a similarly limited role in immune responses against *M. bovis* BCG (32, 33). Furthermore, in challenge studies with *Plasmodium falciparum*, TNFRp75 inhibited protective immune function (34).

To our knowledge, the role of TNFRp75 in virulent *M. tuberculosis* infection has not previously been reported, and whether it promotes or inhibits the protective immune response is still contentious. In the present study, we investigated the respective functions of TNFRp55 and TNFRp75 in protective immunity against *M. tuberculosis* in an aerosol inhalation infection model and explored the mechanisms associated with the increased resistance of TNFRp75-deficient mice to *M. tuberculosis* infection.

Results

TNFRp75-deficient mice are resistant to acute M. tuberculosis infection. We compared tuberculosis disease progression in WT, *Tnfrsf1a*$^{-/-}$ (referred to herein as TNFRp55$^{-/-}$), *Tnfrsf1b*$^{-/-}$ (TNFRp75$^{-/-}$), and double-deficient TNFRp55/75$^{-/-}$ mice upon aerosol infection with *M. tuberculosis* H37Rv at a dose of 50–100 CFU/lung. We recorded survival for the duration of the study and measured weight loss as a clinical correlate of disease progression (Figure 1, A and B). Similar to previous reports of intravenous *M. tuberculosis* infection of TNFRp55$^{-/-}$ mice (24), both TNFRp55$^{-/-}$ and TNFRp55/75$^{-/-}$ mouse strains were highly susceptible to infection, lost significant body weight (≥25% of original body weight), and rapidly succumbed to disease (Figure 1, A and B). A small but consistently higher mortality rate was observed in TNFRp55/75$^{-/-}$ compared with TNFRp55$^{-/-}$ mice (Figure 1A). Conversely, like WT mice, TNFRp75$^{-/-}$ mice were resistant to infection, maintained their body weight, and survived the duration of the experiment (Figure 1, A and B). Therefore, TNFRp55 is critical for protection against *M. tuberculosis* infection, whereas the absence of TNFRp75 did not impair the host response.

We next investigated control of bacilli replication in the mutant strains after *M. tuberculosis* infection. Whereas the WT, TNFRp55$^{-/-}$, and TNFRp55/75$^{-/-}$ strains had comparable pulmonary bacilli burdens up to day 21 after infection, a significantly lower bacilli burden was found in TNFRp75$^{-/-}$ mice (Figure 1C), suggesting improved control of bacilli growth in the absence of TNFRp75. The kinetics of bacilli replication reflected increasing bacilli levels in all strains until day 21 after infection, after which replication was controlled in WT and TNFRp75$^{-/-}$ mice, but not in TNFRp55$^{-/-}$ or TNFRp55/75$^{-/-}$ mice, which reached significance relative to WT values at 28, 35, and 40 days after infection (P < 0.01; Figure 1C). Furthermore, the absence of both TNFRs rendered mice more susceptible, with significantly higher bacilli burdens recorded in TNFRp55/75$^{-/-}$ versus TNFRp55$^{-/-}$ mice at 28, 35, and 40 days after infection (P < 0.05; Fig-

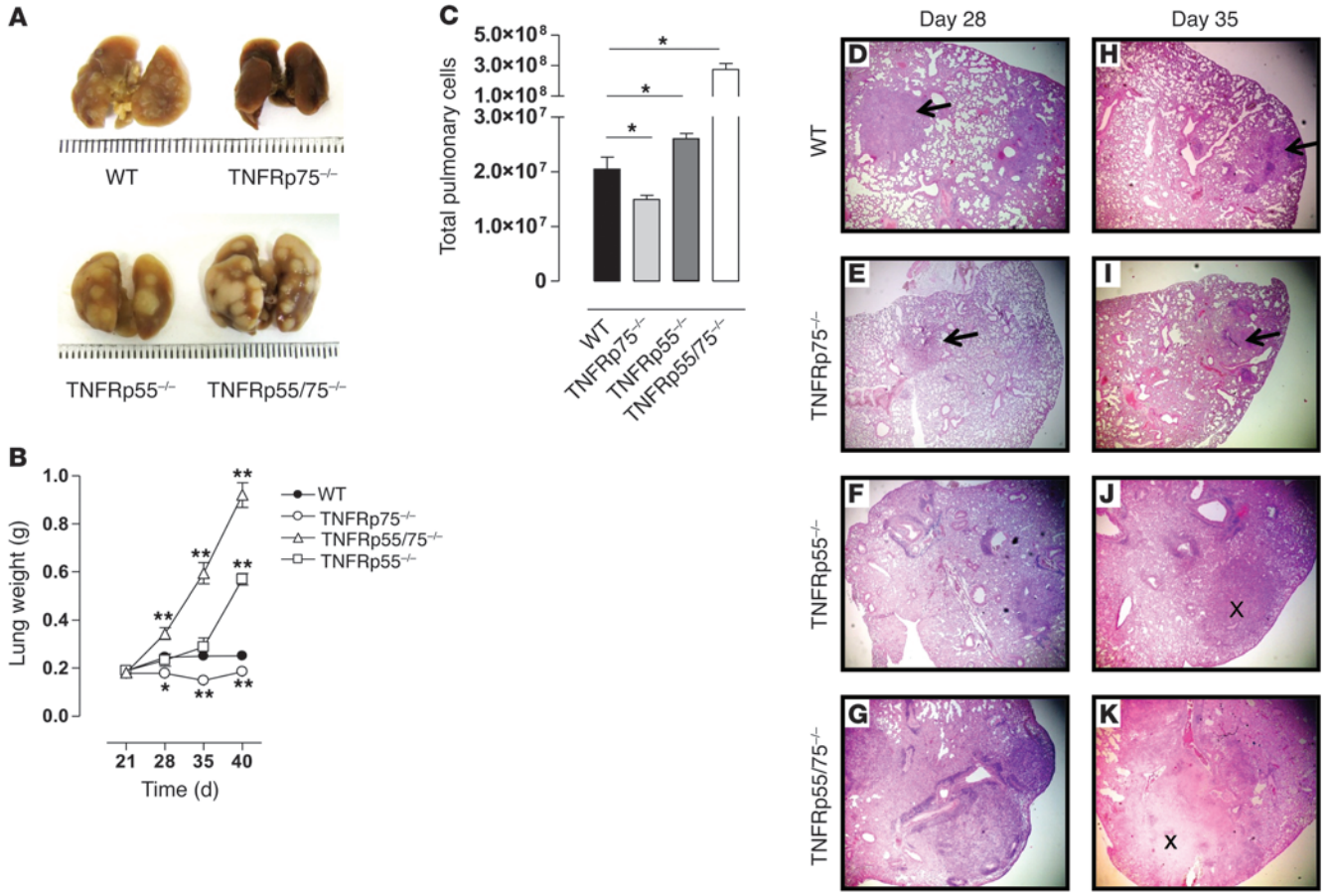

Figure 2
Reduced pulmonary pathology and inflammation in *M. tuberculosis*–infected TNFRp75$^{-/-}$ mice. WT, TNFRp75$^{-/-}$, TNFRp55$^{-/-}$, and TNFRp55/75$^{-/-}$ mice were infected by aerosol inhalation with 50–100 CFU *M. tuberculosis*. Mice were sacrificed at the indicated time points, pulmonary pathology was recorded 35 days after infection (**A**), lung weights were assessed (**B**), and total pulmonary cell numbers at day 35 after infection were determined (**C**). Values are mean ± SEM of 4 mice per group. (**D**–**K**) Lungs were removed on days 28 (**D**–**G**) and 35 (**H**–**K**), fixed in formalin, embedded in wax, and sectioned, after which H&E staining was performed. Arrows denote the presence of granuloma structures; × symbols denote tissue necrosis. Original magnification, ×40. Data represent 1 of 3 similar experiments. *$P < 0.05$, **$P < 0.01$, ANOVA.

ure 1C). A striking and unexpected observation was the maintenance of a significantly lower pulmonary bacilli burden in TNFRp75$^{-/-}$ versus WT mice at each time point tested ($P < 0.01$; Figure 1C). Similarly reduced bacilli burdens were also observed at extrapulmonary sites in TNFRp75$^{-/-}$ mice during chronic infection (Supplemental Figure 1; supplemental material available online with this article; doi:10.1172/JCI45005DS1). This enhanced bacilli control suggested that TNFRp75 may have an adverse role in host protective immune responses against pulmonary *M. tuberculosis* infection.

TNFRp75 expression has a limited effect on M. tuberculosis–induced granuloma formation. Granuloma formation is dependent on signaling of TNF through TNFRp55 in response to *M. tuberculosis* challenge (9); the role of TNFRp75 in this process is undefined. We therefore investigated the effect of TNFRp75 on pulmonary induced pathology: first macroscopically to analyze gross effects, then at a microscopic level to assess cellular responses. Small but distinct lesions were observed on the pleura of WT mice, whereas TNFRp55$^{-/-}$ and TNFRp55/75$^{-/-}$ mice displayed notably enlarged pulmonary lesions at day 35 after infection, with the most severe phenotype evident in TNFRp55/75$^{-/-}$ mice (Figure 2A). In contrast, limited lesion formation was visible in pleura of TNFRp75$^{-/-}$ mice. We next measured lung weight as a surrogate marker of inflammation and found similar weights in all mouse strains until 21 days after infection (Figure 2B). However, in the absence of complete TNFR signaling, TNFRp55/75$^{-/-}$ mice developed an early, uncontrolled inflammatory response, with significantly higher lung weights already evident at 28 days after infection compared with any other strain ($P < 0.01$; Figure 2B), an effect that was sustained for the duration of the study. Lung inflammation in TNFRp55$^{-/-}$ mice was delayed relative to TNFRp55/75$^{-/-}$ mice, but significantly higher lung weights compared with WT mice were nevertheless measured at 40 days after infection ($P < 0.01$; Figure 2B). In contrast, inflammation in TNFRp75$^{-/-}$ mice was significantly lower than their WT counterparts at 28, 35, and 40 days after infection ($P < 0.01$; Figure 2B). The observed differences in inflammation were verified by comparative measurements of the total number of lung cells in infected mice at 35 days after infection (Figure 2C).

To investigate the influence of TNFRp75 on granuloma formation, we analyzed morphology of lung tissue sections in WT, TNFRp55$^{-/-}$, TNFRp75$^{-/-}$, and TNFRp55/75$^{-/-}$ mice and

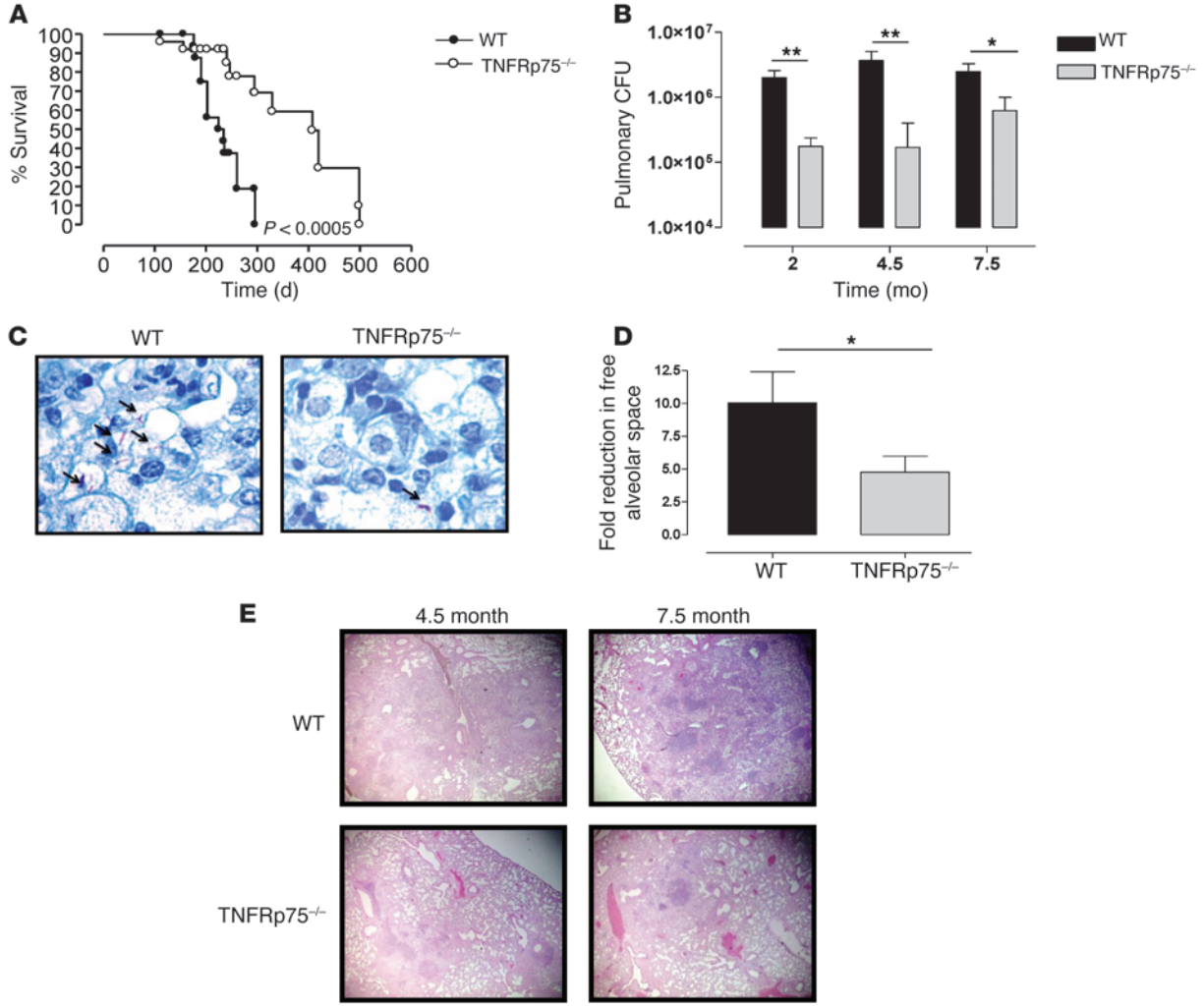

Figure 3

Increased protection of TNFRp75$^{-/-}$ mice during chronic *M. tuberculosis* infection. WT and TNFRp75$^{-/-}$ mice were infected by aerosol inhalation with 50–100 CFU *M. tuberculosis*. (**A** and **B**) Survival was monitored (**A**; n = 10 per group; $P < 0.0005$, log-rank test), and pulmonary bacilli burdens were determined at the indicated time points by colony enumeration assay (**B**). (**C**) Bacilli burden in lung sections was confirmed by Ziehl-Neelsen staining. (**D** and **E**) Chronic inflammation was quantified at 4.5 months after infection (**D**) and confirmed by analysis of H&E-stained lungs sections at 4.5 and 7.5 months after infection (**E**). Original magnification, ×1,000 (**C**); ×40 (**E**). Values in **B** and **D** are mean ± SEM of 4 mice per group. Data are representative of 4 similar experiments (**A**) or 1 of 3 similar experiments (**B**–**E**). *$P < 0.05$, **$P < 0.01$, ANOVA.

compared development at 14, 28, and 35 days after *M. tuberculosis* infection. Lung morphology was largely indistinguishable at 14 days after infection, characterized by intact alveoli and clear bronchi in all strains (data not shown). However, a clear distinction in granuloma structural organization was evident at days 28 and 35 after infection between mice that expressed TNFRp55 and mice in which the receptor was absent (Figure 2, D–K). We observed clearly demarcated granuloma structures, consisting of epithelioid macrophages interspersed with lymphocytes, in WT and TNFRp75$^{-/-}$ mice; conversely, TNFRp55$^{-/-}$ and TNFRp55/75$^{-/-}$ mice were devoid of such organized structures and had noticeable areas of necrosis. Interestingly, granulomas of TNFRp75$^{-/-}$ mice appeared to be smaller than those generated by WT mice (Figure 2, D, E, H, and I). Therefore, our data support a regulatory role for TNFRp55 in the control of pulmonary inflammation and granuloma formation and a dual role for TNFRp75: mediating exacerbation of pulmonary inflammation in the presence of TNFRp55, while enhancing control of inflammation in its absence.

Enhanced protective immunity is maintained, and survival of TNFRp75$^{-/-}$ mice is increased, during chronic M. tuberculosis infection. We next assessed whether the enhanced protective phenotype we observed in the absence of TNFRp75 translates to improved outcome during chronic *M. tuberculosis* infection. WT and TNFRp75$^{-/-}$ mice were infected with *M. tuberculosis*, and pulmonary bacilli burden was determined and mortality recorded. Survival of TNFRp75$^{-/-}$ mice was significantly longer than that of their WT counterparts, a result that was associated with significantly lower bacilli levels at 2, 4.5, and 7.5 months after infection (Figure 3, A and B). The reduced pulmonary bacilli burdens in TNFRp75$^{-/-}$ lungs were confirmed visually by Ziehl-Neelsen staining of tissue sections (Figure 3C). Finally, increased inflammation was verified by quantification of

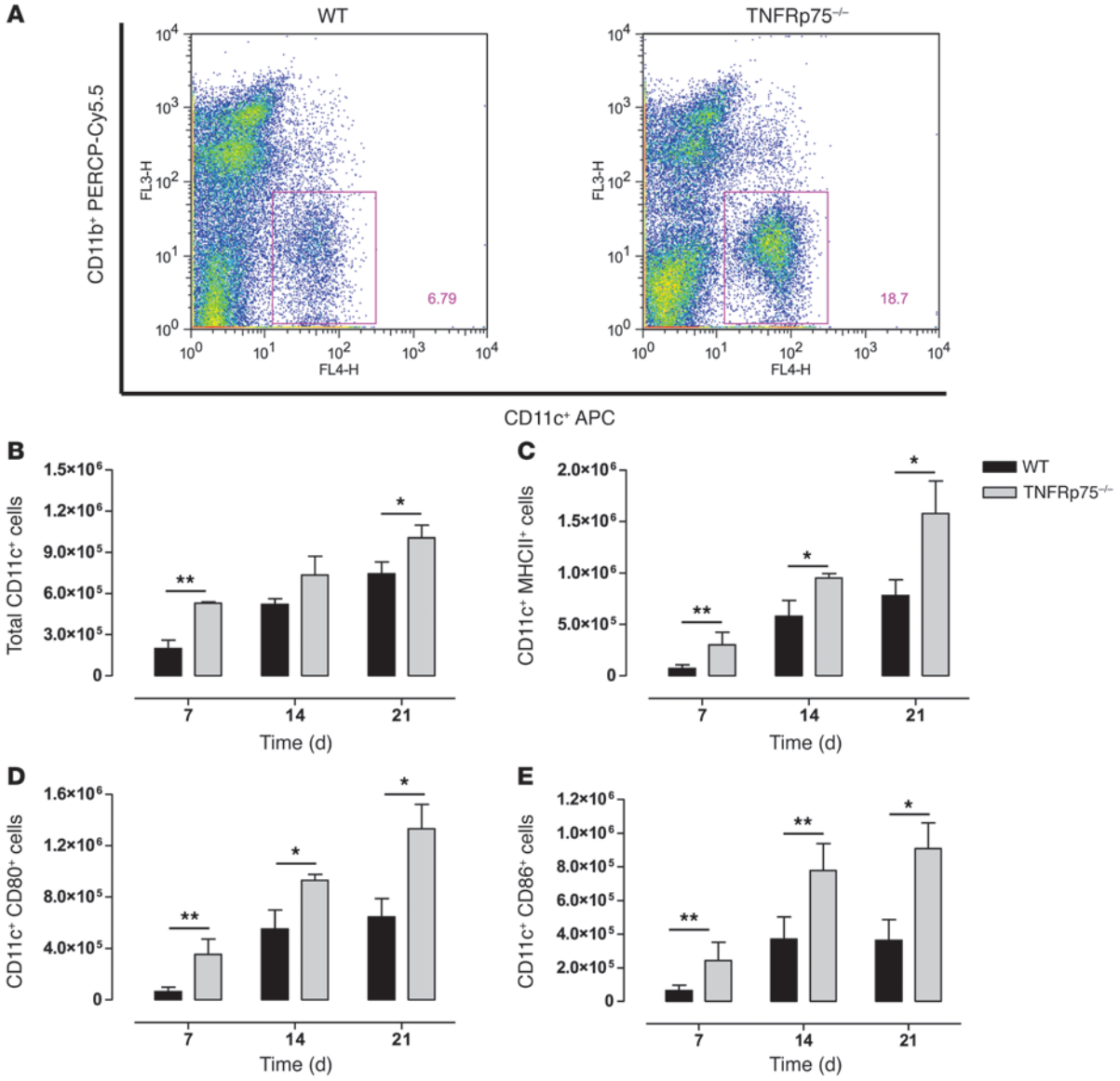

Figure 4

Increased recruitment of activated DCs to the lungs of *M. tuberculosis*–infected TNFRp75$^{-/-}$ mice. WT and TNFRp75$^{-/-}$ mice were infected at 50–100 CFU with *M. tuberculosis*. Lungs were harvested at 7, 14, and 21 days after infection, and CD11b^{+} versus CD11c^{+} cell distribution (**A**) and total number of CD11c^{+} (**B**), CD11c^{+}MHCII^{+} (**C**), CD11c^{+}CD80^{+} (**D**), and CD11c^{+}CD86^{+} (**E**) cells was assessed by flow cytometry. Data (mean ± SEM of 4 mice per group) are representative of 1 of 2 similar experiments. *$P < 0.05$, **$P < 0.01$, ANOVA.

free alveolar space at 4.5 months after infection, which showed a significant increase in occlusion in WT versus TNFRp75$^{-/-}$ mice ($P < 0.05$; Figure 3D). This was confirmed by analysis of lung tissue sections: pathology was characterized by higher cellular infiltration in WT versus TNFRp75$^{-/-}$ mice at both 4.5 and 7.5 months after infection (Figure 3E). Therefore, the early protection observed during acute infection in TNFRp75$^{-/-}$ mice translated to an enhanced protective outcome of disease.

Increased pulmonary recruitment of activated DCs in TNFRp75$^{-/-}$ mice during M. tuberculosis infection. To understand the immune mechanisms associated with the increased protection observed in *M. tuberculosis*–infected TNFRp75$^{-/-}$ mice, we asked whether TNFRp75 regulates immune function through recruitment and/or activation of antigen-presenting cells. WT and TNFRp75$^{-/-}$ mice were infected with *M. tuberculosis*, and DCs (CD11b^{int}CD11c^{+}) were evaluated after 7, 14, and 21 days in the lungs, and cellular activation was assessed by expression of CD80, CD86, and MHCII (Figure 4, A–E). The total number of DCs recruited to the lungs was significantly higher in TNFRp75$^{-/-}$ mice 7 and 21 days after infection ($P < 0.01$ and $P < 0.05$, respectively; Figure 4B). Moreover, the number of recruited pulmonary DCs expressing MHCII, CD80, or CD86 were significantly higher in TNFRp75$^{-/-}$ compared with WT mice after 7, 14, and 21 days (Figure 4, C–E). Together, these data confirmed that TNFRp75 regulates early recruitment and activation of DCs to the lungs during *M. tuberculosis* infection.

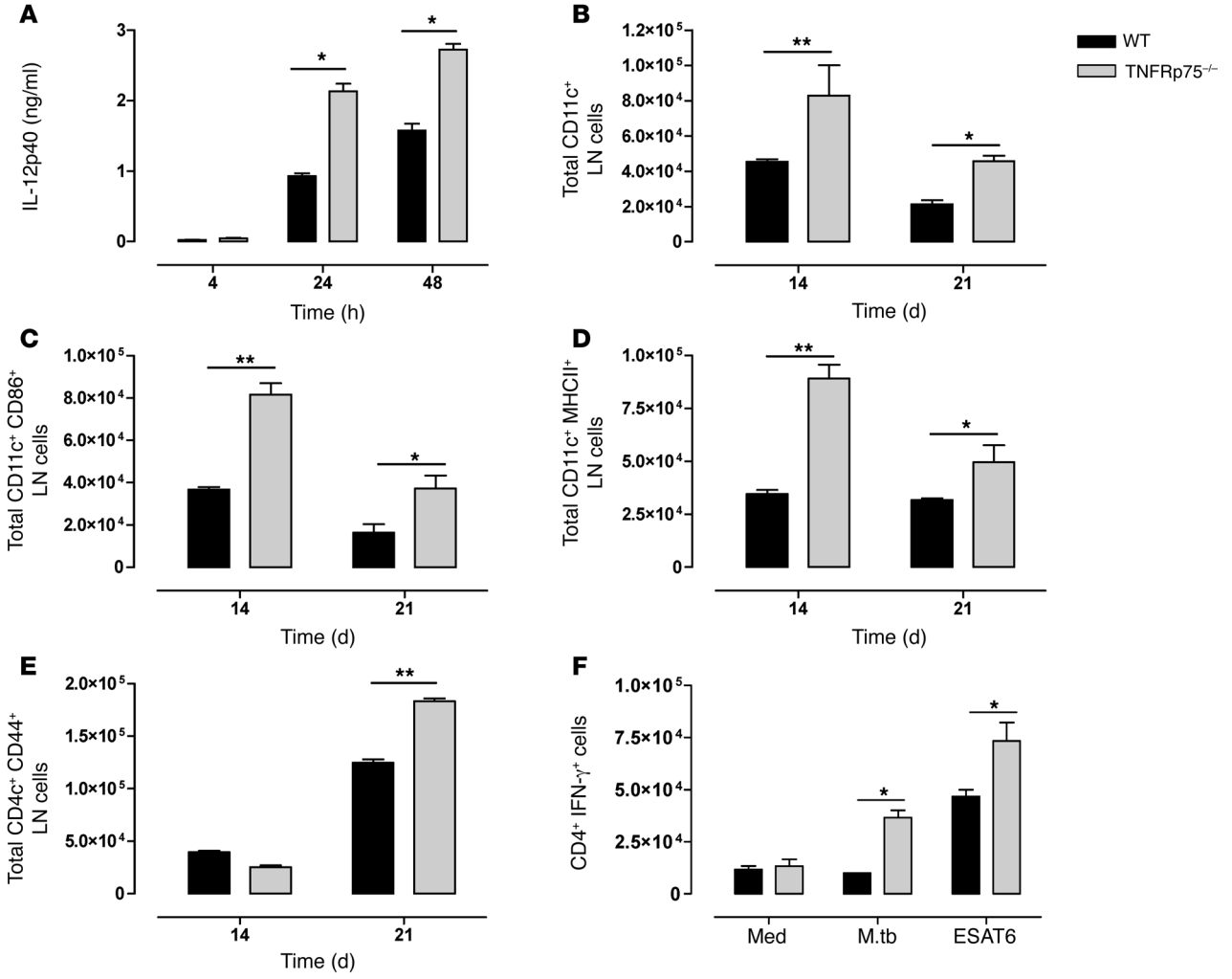

Figure 5
Increased activated DCs induces enhanced *M. tuberculosis*–specific IFN-γ production by activated CD4+ T cells in *M. tuberculosis*–infected TNFRp75$^{-/-}$ mice. (**A**) BMDCs from WT and TNFRp75$^{-/-}$ mice were infected at an MOI of 5:1 with *M. tuberculosis*, and IL-12p40 expression in culture supernatants was analyzed by ELISA. (**B**–**E**) WT and TNFRp75$^{-/-}$ mice were infected at 50–100 CFU with *M. tuberculosis*, and lungs and LNs were harvested 14 and 21 days after infection. The total number of LN CD11c+ cells (**B**), CD11c+CD86+ cells (**C**), CD11c+MHCII+ cells (**D**), and CD4+CD44+ T cells (**E**) was analyzed by flow cytometry. Data (mean ± SEM of 4 mice per group) are representative of 3 similar experiments. (**F**) IFN-γ expression by CD4+ T cells in isolated pulmonary cell cultures restimulated with ESAT6 or *M. tuberculosis* H37Rv (M.tb). Data (mean ± SEM of triplicate values of pooled samples from 4 mice) are representative of 3 similar experiments. *$P < 0.05$, **$P < 0.01$, ANOVA.

Enhanced IL-12p40–dependent DC migration is associated with increased recruitment of activated T cells and superior M. tuberculosis–specific Th1 responses in TNFRp75$^{-/-}$ mice. To understand the effect of TNFRp75 on DC function, we measured the capacity of DCs to produce IL-12p40 upon *M. tuberculosis* infection. BM-derived DCs (BMDCs) from WT and TNFRp75$^{-/-}$ mice were exposed to *M. tuberculosis*, and both showed a time-dependent increase in IL-12p40 synthesis (Figure 5A). Interestingly, we found that IL-12p40 synthesis was regulated by TNFRp75, with TNFRp75$^{-/-}$ culture supernatants measuring significantly higher levels at 24 and 48 hours ($P < 0.05$; Figure 5A). We next postulated that because DC-derived IL-12 is important for the migration of DCs to draining LNs (35), TNFRp75-dependent regulation of IL-12 synthesis may influence the DC content of mediastinal LNs during in vivo aerosol *M. tuberculosis* infection. LNs were harvested from WT and TNFRp75$^{-/-}$ mice on days 14 and 21 after infection, and the number of DCs was analyzed by flow cytometry. Indeed, the total number of DCs was significantly higher in TNFRp75$^{-/-}$ versus WT mice (Figure 5B). Moreover, the number of activated DCs expressing CD86 or MHCII was significantly increased in the LNs of TNFRp75$^{-/-}$ mice (Figure 5, C and D). Equivalent expression of caspase-3 in WT and TNFRp75$^{-/-}$ mice confirmed that increased DC content was attributed to enhanced recruitment, rather than differences in apoptosis (Supplemental Figure 2). Together, these data demonstrated that TNFRp75$^{-/-}$ DCs have an increased capacity for IL-12p40 synthesis that promotes increased migration of activated DCs to draining LNs during *M. tuberculosis* infection.

Given that TNFRp75 regulates recruitment and activation of DCs in the mediastinal LNs during *M. tuberculosis* infection, we next asked whether increased recruitment of activated DCs in LNs of TNFRp75$^{-/-}$ mice translates to an enhanced Th1 *M. tuberculosis*–

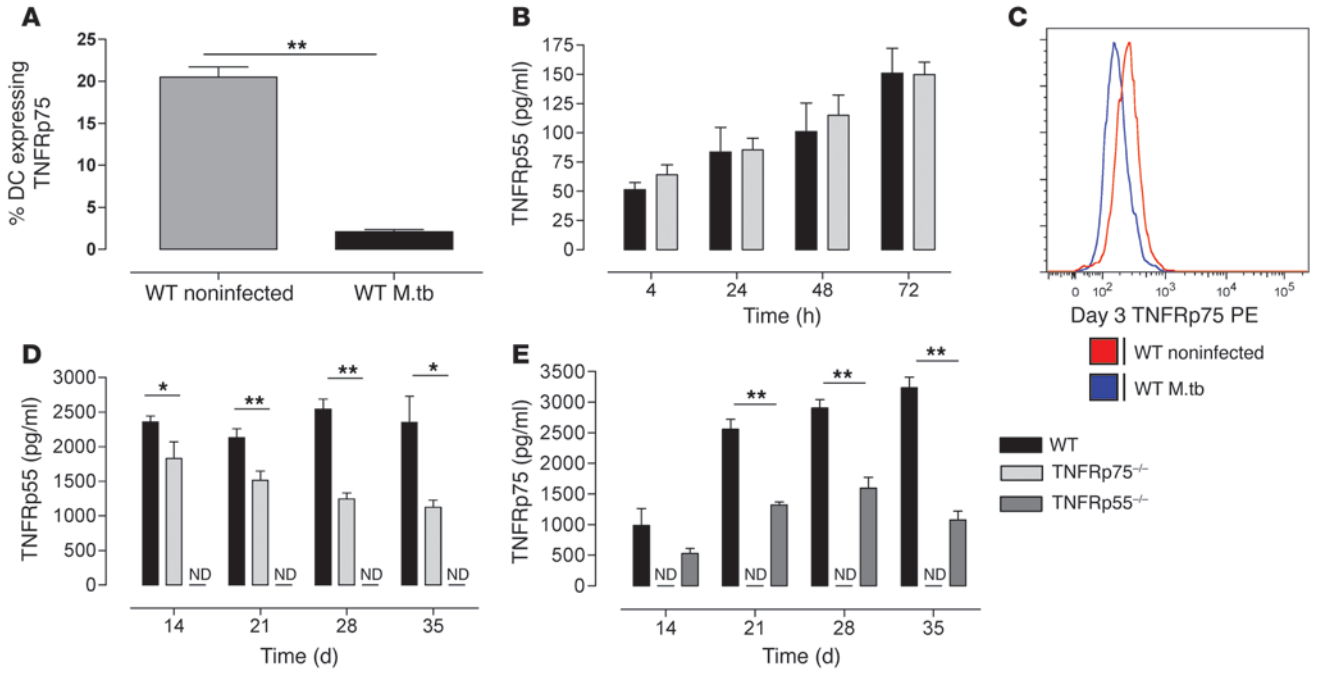

Figure 6

M. tuberculosis induces TNFR shedding. (**A** and **B**) WT and TNFRp75$^{-/-}$ BMDCs were infected with *M. tuberculosis* at an MOI of 5:1, and TNFRp75 surface expression (**A**) and soluble TNFRp55 (**B**) were measured. Data (mean ± SEM of quadruplicate experiments) are representative of 1 of 2 experiments. (**C**–**E**) WT, TNFRp75$^{-/-}$, and TNFRp55$^{-/-}$ mice were infected with 50–100 CFU *M. tuberculosis*. Surface TNFRp75 (**C**) was measured by flow cytometry in BAL cells, and soluble TNFRp55 (**D**) and TNFRp75 (**E**) were measured in lung homogenates by ELISA. ND, not detectable. Data (mean ± SEM of 4–5 mice per group) are representative of 1 of 2 similar experiments. *$P < 0.05$, **$P < 0.01$, ANOVA.

specific immune response. We first compared CD4$^+$ and CD8$^+$ T cell recruitment and activation in the LNs, postulating that the increased number of activated DCs would lead to increased T cell recruitment and activation in the absence of TNFRp75. Quantification of CD4$^+$CD44$^+$ T cells revealed an early increase in recruitment of activated T cells in the TNFRp75$^{-/-}$ LNs (Figure 5E). Similarly, the percentage of CD8$^+$CD44$^+$ T cells was increased in TNFRp75$^{-/-}$ compared with WT mice at day 21 (data not shown). We next evaluated antigen-specific IFN-γ–expressing CD4$^+$ T cells at the sites of infection ex vivo. Low frequencies of IFN-γ–expressing CD4$^+$ T cells were detected in both groups in the absence of antigenic stimuli; however, restimulation with either live *M. tuberculosis* or ESAT6 increased the frequency of IFN-γ–expressing CD4$^+$ pulmonary T cells of TNFRp75$^{-/-}$ mice ($P < 0.05$; Figure 5F). Additionally, we measured IL-10 and IL-13 synthesis as regulators of Th1/Th2 balance (36, 37), where both cytokines can control DC maturation and function (38, 39); however, we found no pulmonary concentration differences between WT and TNFRp75$^{-/-}$ mice during acute or chronic *M. tuberculosis* infection (Supplemental Figure 3). Thus, our data confirmed that the increased recruitment of activated DCs in TNFRp75$^{-/-}$ mice increases the frequency of activated T cells in LNs, with the capability to generate enhanced *M. tuberculosis*–specific immune responses.

TNFRp75 shedding is induced in vivo during M. tuberculosis infection. Previous studies demonstrated that TNFRp55 and TNFRp75 are shed from the cell surface in response to in vitro virulent *M. tuberculosis* H37Rv infection (7) or in vivo *M. avium* infection (6), reducing bioactive TNF. In our studies, flow cytometric analysis of TNFRp75 surface expression in WT DCs revealed a 10-fold reduction in TNFRp75-expressing cells 24 hours after *M. tuberculosis* infection compared with noninfected cells ($P < 0.01$; Figure 6A). Detection of TNFRp75 release in culture supernatants of *M. tuberculosis*–infected WT DCs was assessed to confirm that decreased expression was indeed due to shedding, as opposed to receptor internalization. We observed time-dependent shedding of TNFRp75 in WT DCs, reaching a maximum after 48 hours, and confirmed the absence of TNFRp75 in the TNFRp75$^{-/-}$ cell cultures (Supplemental Figure 4A). Additionally, we compared the kinetics of TNFRp55 shedding in the culture supernatants of *M. tuberculosis*–infected DCs of WT and TNFRp75$^{-/-}$ mice and found that *M. tuberculosis* infection induced an increase in TNFRp55 release over 72 hours in both strains (Figure 6B).

To ascertain whether the *M. tuberculosis*–induced TNFR shedding we observed in vitro also occurs in vivo, we challenged WT, TNFRp55$^{-/-}$, and TNFRp75$^{-/-}$ mice with *M. tuberculosis* and assessed TNFRp55 and TNFRp75 levels in bronchoalveolar lavage fluid (BALF) and supernatants of lung homogenates at defined time points. Flow cytometric analysis of bronchoalveolar lavage (BAL) DCs harvested 3 days after infection showed reduced TNFRp75 expression in *M. tuberculosis*–infected WT versus naive control mice (Figure 6C). We then assessed soluble TNFRp55 and TNFRp75 concentrations in BALF and supernatants of lung homogenates at defined time points to confirm receptor shedding in vivo. We found that TNFRp55 and TNFRp75 were shed subsequent to *M. tuberculosis* infection and confirmed that TNFRp55 and TNFRp75 were not detectable in TNFRp55$^{-/-}$ and TNFRp75$^{-/-}$ mice, respectively (Figure 6, D and E, and Supplemental Figure 4, A–C). Interestingly, we measured lower TNFRp55 levels in

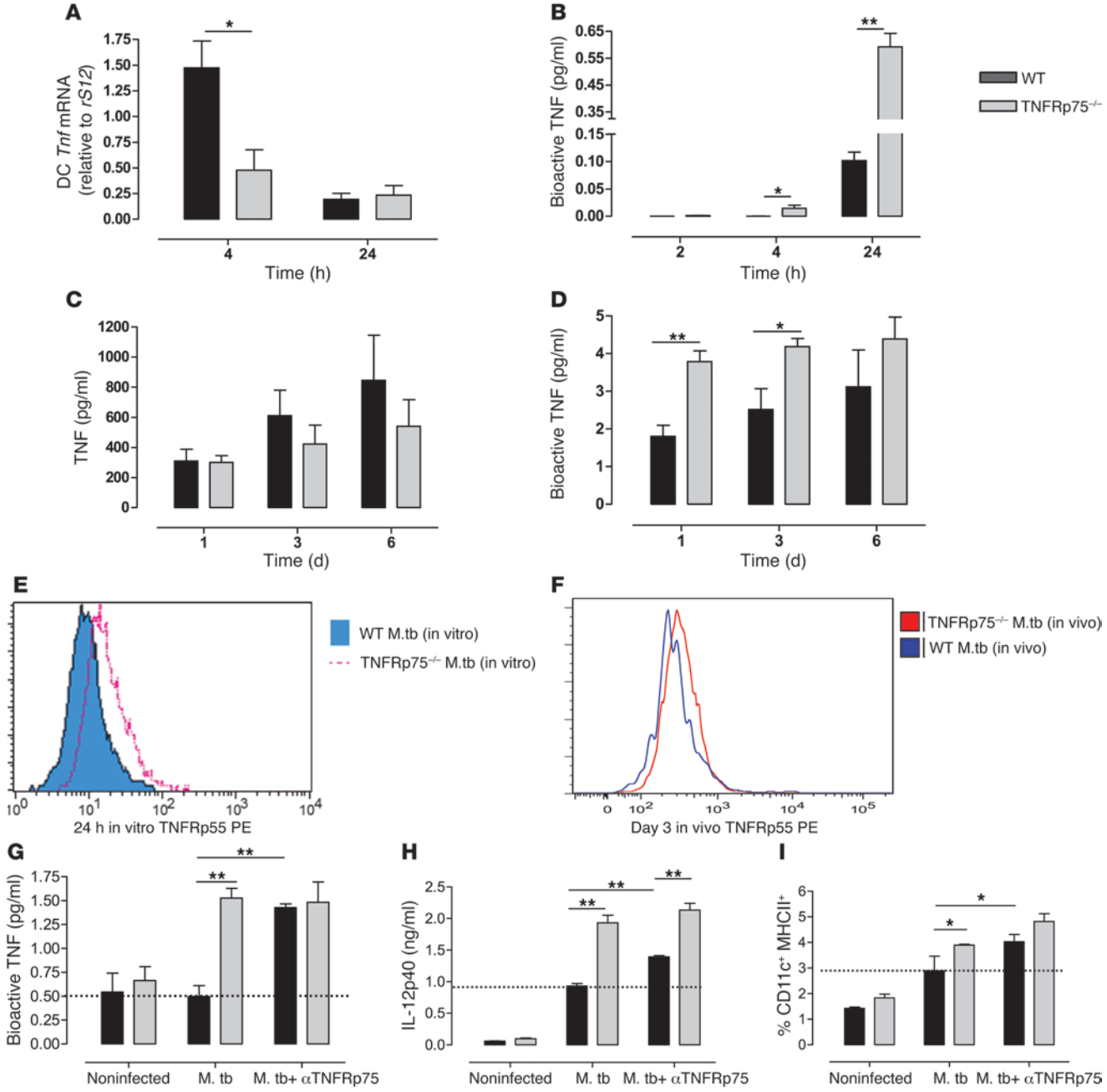

Figure 7

Soluble TNFRp75 inhibits DC activation during *M. tuberculosis* infection. (**A** and **B**) WT and TNFRp75$^{-/-}$ DCs were infected with *M. tuberculosis* at an MOI of 5:1, and *Tnf* mRNA (**A**) or bioactive TNF (**B**) concentrations were measured. (**C** and **D**) WT and TNFRp75$^{-/-}$ mice were infected with 50–100 CFU *M. tuberculosis*. Total (**C**) and bioactive (**D**) TNF was measured in BALF 1, 3, and 6 days after infection. (**E** and **F**) In vitro surface expression of TNFRp55 (**E**) was measured in WT and TNFRp75$^{-/-}$ BMDCs, and in vivo surface TNFRp55 (**F**) was measured by flow cytometry in BAL cells. (**G**–**I**) The effect of soluble TNFRp75 on *M. tuberculosis*–infected BMDC cultures from WT and TNFRp75$^{-/-}$ mice were assessed by measuring bioactive TNF (**G**), IL-12p40 (**H**), and MHCII^{+} expression (**I**) in the presence or absence of anti-TNFRp75. Note the increased expression induced by anti-TNFRp75 in WT mice compared with *M. tuberculosis* infection alone (dashed lines). Data (mean ± SEM of quadruplicate experiments) are representative of 1 of 2 similar experiments. *$P < 0.05$, **$P < 0.01$, ANOVA.

TNFRp75$^{-/-}$ versus WT mice at all time points, which suggests that TNFRp75 may regulate TNFRp55 shedding. Furthermore, shedding of TNFRp75 was significantly lower in TNFRp55$^{-/-}$ versus WT mice ($P < 0.01$). These data demonstrated that both TNFRp55 and TNFRp75 are shed during host challenge with *M. tuberculosis* and that TNFR shedding seems to be regulated by signaling through the opposing TNFR.

Neutralization of TNFRp75 increases DC activation. We hypothesized that TNFRp75 shedding would regulate bioactive TNF concentrations and thus early host immune responses. Therefore, WT and

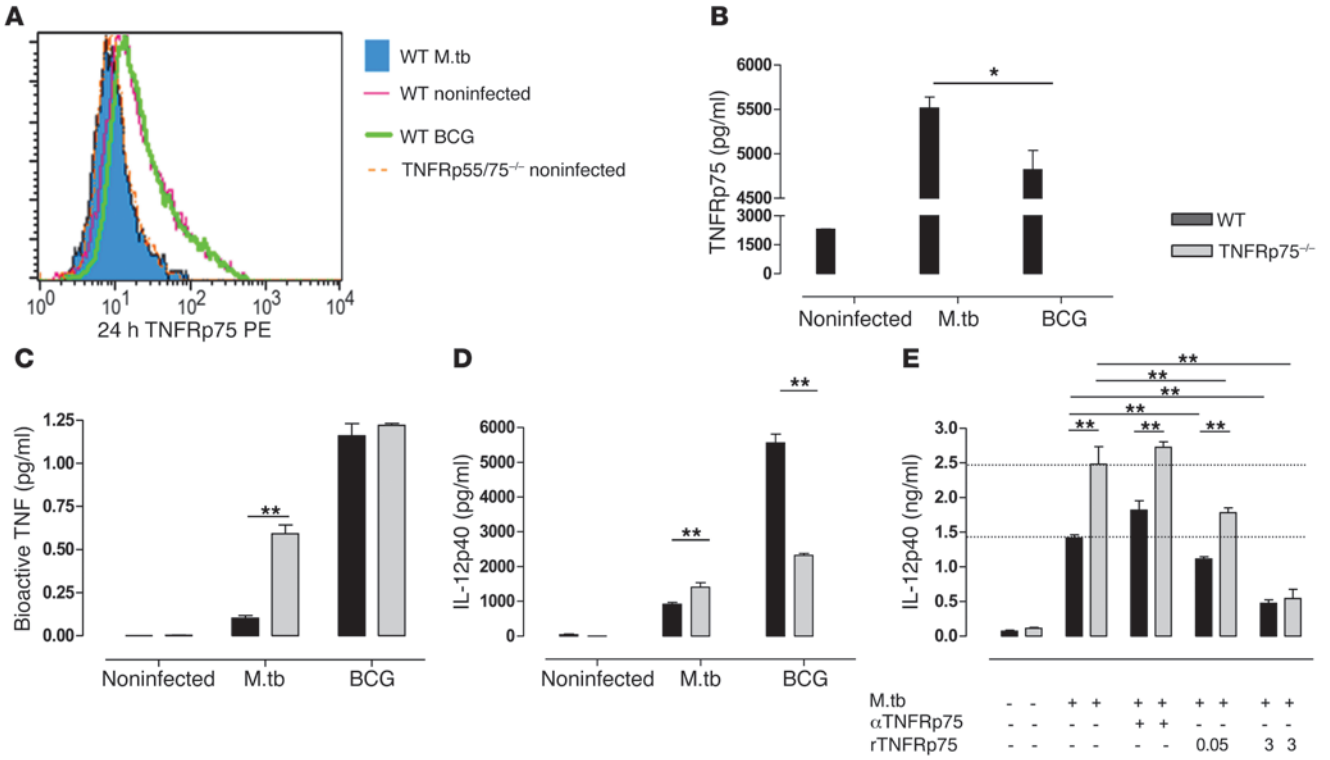

Figure 8

DC activation is dependent on soluble TNFRp75 inactivation of bioactive TNF. (**A**–**D**) WT, TNFRp75$^{-/-}$, and TNFRp55/75$^{-/-}$ BMDCs were infected with *M. tuberculosis* or *M. bovis* BCG at an MOI of 5:1. Surface expression of TNFRp75 (**A**), soluble TNFRp75 (**B**), bioactive TNF (**C**), and IL-12p40 (**D**) was measured. (**E**) The effect of recombinant TNFRp75 on *M. tuberculosis*–infected BMDC cultures from WT and TNFRp75$^{-/-}$ mice were assessed by measuring IL-12p40 in the presence or absence of recombinant TNFRp75. Whereas anti-TNFRp75 in WT mice increased IL-12p40 expression, addition of recombinant TNFRp75 dose-dependently reduced expression in both WT and TNFRp75$^{-/-}$ mice, compared with *M. tuberculosis* infection alone (dashed lines). Data (mean ± SEM of quadruplicate experiments) are representative of 1 of 2 similar experiments. *$P < 0.05$, **$P < 0.01$, ANOVA.

TNFRp75$^{-/-}$ cultured DCs were infected with *M. tuberculosis* at an MOI of 5:1 in the presence or absence of anti-TNFRp75 and bioactive TNF, and expression of IL-12p40 and MHCII (as indicators of DC activation) was measured. In addition, *Tnf* mRNA expression, bioactive TNF kinetics, and DC surface TNFRp55 expression were analyzed. Although *Tnf* mRNA expression was significantly reduced in TNFRp75$^{-/-}$ BMDCs ($P < 0.05$; Figure 7A), bioactive TNF was significantly higher at 4 and 24 hours after infection ($P < 0.05$ and $P < 0.01$, respectively; Figure 7B). In addition, we measured and compared pulmonary total TNF and bioactive TNF concentrations in *M. tuberculosis*–infected WT and TNFRp75$^{-/-}$ mice at 1, 3, and 6 days after infection. We found equivalent total TNF concentrations, as opposed to significantly higher bioactive TNF concentrations in TNFRp75$^{-/-}$ versus WT mice at 1 and 3 days after infection ($P < 0.05$; Figure 7, C and D).

We next postulated that the increased bioactive TNF concentrations would have enhanced potential for DC activation via TNFRp55 signaling in the absence of TNFRp75. Flow cytometric analysis revealed upregulation of TNFRp55 in TNFRp75$^{-/-}$ BMDCs (Figure 7E). This was strongly supported by analysis of pulmonary DCs showing increased TNFRp55 cell surface expression in *M. tuberculosis*–infected TNFRp75$^{-/-}$ compared with WT mice at 3 days after infection (Figure 7F). TNFRp75-dependent regulation of TNF bioactivity was confirmed in studies where treatment of WT DC cultures with anti-TNFRp75 neutralizing antibody resulted in a bioactive TNF response similar to that of TNFRp75$^{-/-}$ DCs (Figure 7G). Thus, these findings reinforced the hypothesis that soluble TNFRp75 inhibits bioactive TNF concentrations. Moreover, we observed increased IL-12p40 production and MHCII expression in *M. tuberculosis*–infected TNFRp75$^{-/-}$ DCs (Figure 7, H and I), confirming enhanced DC activation. Treatment of WT DC cultures with anti-TNFRp75 neutralizing antibody lead to significant increases in IL-12p40 and MHCII expression ($P < 0.01$ and $P < 0.05$, respectively; Figure 7, H and I), approaching — albeit not equivalent to — levels of TNFRp75$^{-/-}$ DCs. Taken together, these data support a heightened activated phenotype of TNFRp75$^{-/-}$ compared with WT DCs after *M. tuberculosis* infection, mediated by enhanced signaling of bioactive TNF through TNFRp55. Notably, neutralization studies confirmed that the increased immune function potential of DCs was TNFRp75 dependent.

Soluble TNFRp75 inhibition of bioactive TNF regulates Th1-specific immunity. We postulated that improved protection observed in TNFRp75$^{-/-}$ mice could either be attributed to (a) loss of signaling though TNFRp75, assuming that TNFRp75-mediated signaling downmodulates protective Th1 immunity, or (b) absent TNFRp75 shedding and the resultant bioactive TNF increase mediating an improved Th1-specific immune response. Previous studies

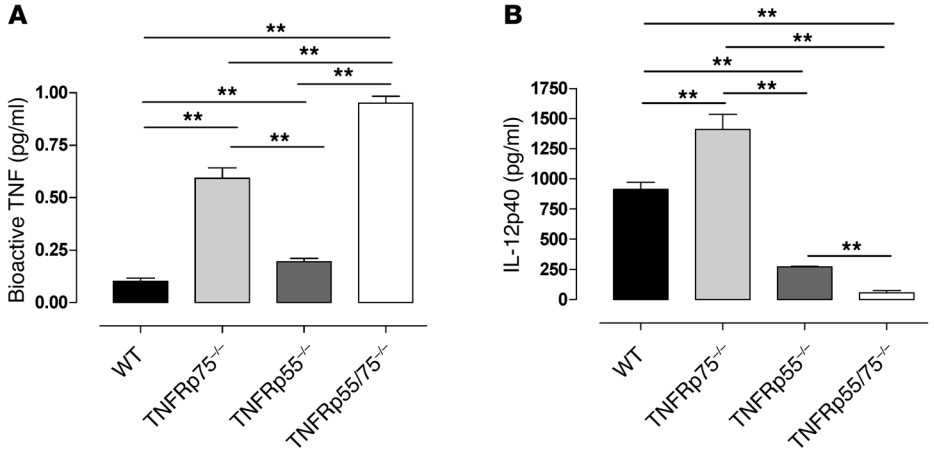

Figure 9
DC activation is primarily mediated by TNF-TNFRp55 signaling and regulated by soluble TNFRp75. WT, TNFRp75$^{-/-}$, TNFRp55$^{-/-}$, and TNFRp55/75$^{-/-}$ DCs were infected with *M. tuberculosis* at an MOI of 5:1. (**A**) Bioactive TNF was determined using WEHI assays. (**B**) IL-12p40 was analyzed by ELISA. Data (mean ± SEM of quadruplicate values) are representative of 1 of 2 similar experiments. $^{**}P < 0.01$, ANOVA.

have demonstrated that TNFRp75 shedding is strain dependent and associated with virulence (7). Therefore, we predicted that TNFRp75 shedding would be less efficient in an attenuated BCG mycobacterial infection model, allowing us to test whether enhanced Th1 immunity in TNFRp75$^{-/-}$ mice is dependent on soluble TNFRp75 and the associated increase in bioactive TNF.

Indeed, we found that BMDCs infected with BCG had TNFRp75 cell surface expression equivalent to that of uninfected BMDCs (Figure 8A). In contrast, BMDCs infected with *M. tuberculosis* exhibited a reduced TNFRp75 MFI (Figure 8A), indicative of loss of cell surface expression, which confirmed that BCG is less efficient at inducing TNFRp75 shedding. The presence of increased soluble TNFRp75 in BMDC culture supernatants confirmed that the loss of surface expression of TNFRp75 was due to receptor shedding, as opposed to receptor internalization (Figure 8B). Although BCG induced low levels of soluble TNFRp75, concentrations remained significantly reduced compared with those induced by *M. tuberculosis* ($P < 0.05$; Figure 8B). More importantly, bioactive TNF concentrations were equivalent in WT and TNFRp75$^{-/-}$ BMDC culture supernatants after BCG challenge, whereas they were significantly increased after virulent *M. tuberculosis* infection ($P < 0.01$; Figure 8C). Since WT and TNFRp75$^{-/-}$ DCs produced similar levels of bioactive TNF during BCG challenge, we assessed IL-12p40 production as a measure of cellular activation and found that the increase in IL-12p40 observed in TNFRp75$^{-/-}$ BMDCs during *M. tuberculosis* infection did not occur during BCG infection, for which receptor shedding was absent. In fact, during BCG infection, WT BMDCs produced significantly increased IL-12p40 compared with TNFRp75$^{-/-}$ BMDCs ($P < 0.01$; Figure 8D). This suggests that TNFRp75 signaling, rather than being inhibitory, acts in concert with TNFRp55 to induce optimal immune activation.

In order to confirm that soluble TNFRp75 and not membrane-bound TNFRp75 signaling impairs immune responses in WT mice, *M. tuberculosis*–infected TNFRp75$^{-/-}$ BMDCs were treated with recombinant TNFRp75 so that experimental conditions approximated the TNFRp75 shedding observed in WT mice in the absence of TNFRp75 signaling. Strikingly, we found a dose-dependent reduction of DC activation with increasing exogenous recombinant TNFRp75 administration (Figure 8E). Taken together, these data confirmed that TNFRp75 shedding and the resulting reduction in bioactive TNF, not TNFRp75-mediated signaling effects, downmodulates DC activation and influences disease outcome.

TNF-TNFRp55–dependent DC activation is critical for M. tuberculosis–specific Th1 immunity. Our data demonstrated a positive correlation between bioactive TNF concentrations and IL-12p40 synthesis during DC exposure to *M. tuberculosis*. To investigate the relative contribution of the respective receptors in TNF-mediated DC activation, we analyzed bioactive TNF and IL-12p40 in WT, TNFRp55$^{-/-}$, TNFRp75$^{-/-}$, and TNFRp55/75$^{-/-}$ BMDCs during *M. tuberculosis* infection. TNFRp75 shedding affected bioactive TNF levels more profoundly than TNFRp55, with TNFRp75$^{-/-}$ BMDCs producing significantly increased bioactive TNF compared with TNFRp55$^{-/-}$ BMDCs ($P < 0.01$; Figure 9A). However, TNFRp55 also contributed to inhibition, since bioactive TNF concentrations were significantly higher in supernatants from TNFRp55$^{-/-}$ versus WT BMDCs ($P < 0.01$; Figure 9A). The contribution of both receptors to inhibition of bioactive TNF was confirmed in TNFRp55/75$^{-/-}$ BMDCs, which had the highest concentrations of bioactive TNF. Interestingly, our data suggested an additive inhibitory effect by the 2 receptors.

Investigation of IL-12p40 synthesis showed that significantly higher concentrations were produced by TNFRp75$^{-/-}$ versus WT BMDCs ($P < 0.01$; Figure 9B). The absence of TNFRp55 significantly reduced IL-12p40 synthesis in both TNFRp55$^{-/-}$ and TNFRp55/75$^{-/-}$ BMDCs. Interestingly, the absence of both TNFRs resulted in near-complete abrogation of IL-12p40 synthesis. Therefore, our data demonstrated that shedding of both TNFRs contributes to inhibition of bioactive TNF, with soluble TNFRp75 playing the predominant role. Although both TNFRs can mediate activation of DCs, TNFRp55 signaling is absolutely critical and superior to TNFRp75 signaling.

Discussion

Although TNF and TNFRp55 are critical for protective immune responses against *M. tuberculosis*, the role of TNFRp75 was unknown. In the current study, we investigated the effects of TNFRp75, under conditions in which TNFRp55 was either expressed or absent, during *M. tuberculosis* challenge. Our results demonstrated that soluble TNFRp75 reduces bioactive TNF concentrations, downmodulates DC activation, and impairs overall Th1 immune responses, whereas membrane TNFRp75 promotes immune protection.

First, we confirmed that TNFRp55 is critical for survival: both TNFRp55$^{-/-}$ and TNFRp55/75$^{-/-}$ mice succumbed to infection, showing increased organ burdens and concomitant weight loss,

both well-documented symptoms of advanced disease. Interestingly, we observed a small but repeatable delay in the death of TNFRp55$^{-/-}$ compared with TNFRp55/75$^{-/-}$ mice, suggestive of a possible degree of protection afforded by TNFRp75 in the absence of TNFRp55. Nonetheless, TNFRp55-mediated immune function was nonredundant and could not be rescued by TNFRp75 expression. In contrast, survival during chronic infection was significantly longer in TNFRp75$^{-/-}$ than WT mice, which suggests that TNFRp75 expression inhibits immune function during *M. tuberculosis* challenge. TNFRp75-dependent inhibition of host immune function during *M. avium* challenge was previously reported by Corti et al., who demonstrated immune benefit associated with TNFRp75 neutralization (6). Furthermore, Balcewicz-Sablinska et al. reported that TNFRp75 shedding is an important *M. tuberculosis* evasion mechanism, particularly in virulent strains (7). Using human alveolar macrophages, the authors found that virulent *M. tuberculosis* H37Rv bacilli were able to evade apoptosis through IL-10–dependent TNFRp75 shedding, while avirulent *M. tuberculosis* H37Ra induced less TNFRp75 shedding, reducing efficiency at evading apoptosis. TNFRp75 could form complexes with soluble TNF, thereby reducing TNF bioactivity and subsequent TNF-mediated immune responses (7).

Cellular recruitment is essential for protective immunity against mycobacterial infections (9–11, 13, 27), partly due to its importance in granuloma formation, a critical component in host immunity without which mice die prematurely (11, 30). TNF signaling mediates both cellular recruitment and subsequent granuloma formation in response to mycobacterial infections (11, 13, 27): the absence of TNF impairs formation of structured granulomas, with few epithelial macrophages and significant necrosis (9, 10). TNFRp55 signaling has previously been shown — in both *M. tuberculosis* (40) and other infection and inflammatory models (41, 42) — to be important for the activation of NF-κB, which results in the synthesis of proinflammatory cytokines, including TNF. Furthermore, as described in the present study and in previous reports (26, 27), TNFRp55 acts as the major conduit of TNF-mediated function, and an inability to signal through TNFRp55 yielded granuloma defects comparable to those observed with TNF deficiency. In both TNFRp55$^{-/-}$ and TNFRp55/75$^{-/-}$ mice, structured granulomas were absent and few epithelioid macrophages were noted, despite significantly increased pulmonary cell numbers. In addition, severe necrosis was observed in the absence of TNFRp55-mediated signaling. In contrast, we found that the organization of granulomas in TNFRp75$^{-/-}$ mice resembled the ordered structure characteristic of WT granulomas. The fewer, smaller granulomas and reduced cell numbers we observed in TNFRp75$^{-/-}$ mice late in the acute stage of infection could be attributed to a reduced stimulus resulting from a lower bacilli burden in this strain, not an inability to recruit immune cells or form granulomas at the site of infection. In fact, TNFRp75$^{-/-}$ mice have an enhanced Th1 immune response during early acute infection. Therefore, our findings, together with other reported studies (9, 10), indicate that TNF signaling through TNFRp55 — and not TNFRp75 — is important for granuloma formation.

To understand the immune mechanisms conferring increased protection in TNFRp75$^{-/-}$ mice, we explored the effects of TNFRp75 on cellular responses during *M. tuberculosis* infection, with particular emphasis on DCs as an integral component of early defense (43) and an important link between innate and adaptive immunity (44, 45). During early acute infection, TNFRp75$^{-/-}$ mice presented with an increase in the number of activated CD11c^{+} DCs in the lungs, which were characterized by CD80, CD86, and MHCII expression and enhanced IL-12p40 synthesis compared with WT mice. DCs are ideally positioned to contribute to both innate and adaptive immune control. Their role in early innate immune defense has been illustrated by others who found that DCs restrict bacterial replication during early infection (46). It is therefore plausible that early protection in TNFRp75$^{-/-}$ mice may be associated with enhanced bacterial control related to the increased number of activated DCs in the absence of TNFRp75. The capacity of DCs to establish innate immune control of bacterial infection via TNF/iNOS-dependent mechanisms has previously been reported (47). The potential for superior killing by the increased DC population in the absence of TNFRp75 remains to be defined. In addition to its role in Th1 polarization, DC-derived IL-12 plays a significant role in the migration of DCs to the draining LNs (35), and our present results confirmed that higher IL-12p40 induction mediated an increase in DC migration to draining LNs in *M. tuberculosis*–infected TNFRp75$^{-/-}$ mice. T cell activation relies primarily on antigen presentation by DCs in the LN, not the lung, during *M. tuberculosis* infection (45), and cytokines such as IL-12 are required to induce Th1 polarization (48–50). Enhanced mycobacterial clearance was associated with increased recruitment of *M. tuberculosis*–specific Th1 cells in the absence of TNFRp75. Interestingly, delayed DC trafficking to LNs hinders timely induction of protective immune responses and alters disease outcome (51). Our results showed enhanced DC migration to LNs in TNFRp75$^{-/-}$ mice, which suggests that soluble TNFRp75 may delay DC trafficking to LNs and impede optimal induction of T cell–mediated immunity. The increased number of activated DCs and increased IL-12p40 in TNFRp75$^{-/-}$ mice would therefore suggest favorable conditions in the LN for T cell activation. Indeed, we noted an increased number of activated CD4^{+}CD44^{+} and CD8^{+}CD44^{+} T cells in the LNs of TNFRp75$^{-/-}$ mice. We also confirmed that newly activated T cells were in fact Th1 polarized, capable of producing IFN-γ once recruited to the lungs. Ex vivo restimulation of lung cells from TNFRp75$^{-/-}$ mice demonstrated an increased ability to generate an *M. tuberculosis*–specific IFN-γ response to ESAT6 or *M. tuberculosis* H37Rv compared with WT mice. Therefore, our collective data provide evidence that TNFRp75 regulates the antigen-presenting potential of DCs and the induction of Th1 immune responses during early acute infection.

The clear correlation we demonstrated between increased early Th1 immune responses and control of bacterial replication in TNFRp75$^{-/-}$ mice emphasizes the importance of a strong early proinflammatory response to the outcome of disease. It also suggests a regulatory role of TNFRp75 in buffering excessive immune function in order to limit immune-mediated tissue damage during *M. tuberculosis* infection at the expense of achieving early control of bacilli replication, which would ultimately lead to increased host survival. Interestingly, we observed no pathological damage as a result of the increased early proinflammatory response in TNFRp75$^{-/-}$ mice, which suggests a highly controlled process. Indeed, the early enhanced Th1 response in TNFRp75$^{-/-}$ mice was downmodulated during later stages of infection, when bacilli replication was controlled, which indicates that the response may be stimuli specific.

In vitro human macrophage studies demonstrated TNFRp55 and TNFRp75 release upon *M. tuberculosis* infection in which predominantly soluble TNFRp75, rather than soluble TNFRp55, formed complexes with soluble TNF, thereby reducing TNF bioactivity (7). In addition, TNFRp75 cell surface expression and shedding was increased in response to intraperitoneal *M. avium*

infection (6). Based on the evidence from these studies, we hypothesized that TNFRp55 and TNFRp75 would be released upon *M. tuberculosis* infection, allowing soluble receptors to bind bioactive TNF and thereby reduce the availability of bioactive TNF for signaling via the membrane-bound receptors. TNF and IFN-γ are known key requirements for optimal cellular activation (52), and reduced availability of bioactive TNF could therefore negatively affect DC activation. Assessment of TNFRp55 and TNFRp75 shedding, both in vivo and in vitro, confirmed the release of TNFRp75 from cell surfaces and demonstrated increased levels of soluble TNFRp75 and TNFRp55 in supernatants after *M. tuberculosis* infection, in accordance with previous reports (6, 7). Interestingly, the absence of TNFRp75 was associated with significantly lower soluble TNFRp55. Both in vitro and in vivo analysis of TNFRp55 showed increased surface expression in TNFRp75$^{-/-}$ DC cultures or BAL mouse lung cells, which suggests that TNFRp55 shedding is promoted by TNFRp75. In addition, BALF from TNFRp75$^{-/-}$ mice and supernatants from TNFRp75$^{-/-}$ BMDCs had higher concentrations of bioactive TNF, which could potentially all signal through TNFRp55. This indicated that immune responses in TNFRp75$^{-/-}$ mice were characterized by improved TNF-TNFRp55 signaling, which promoted the early Th1 proinflammatory immune response essential for early control of bacilli replication and was accordingly associated with reduced pulmonary pathology. In support of this concept, TNFRp75 neutralization in *M. tuberculosis*–infected BMDCs increased IL-12p40 and bioactive TNF expression as well as the number of BMDCs expressing MHCII, further indicating that the increased ability of DCs to become activated was due to increased concentrations of bioactive TNF caused by the reduction in soluble TNFR.

Nonetheless, it could be argued that TNF-TNFRp75–mediated signaling inhibits Th1-mediated immunity and that the increased protection observed in TNFRp75$^{-/-}$ mice was the consequence of absent inhibitory signaling through TNFRp75 rather than inhibited bioactive TNF through binding of soluble TNFRp75. To explore this option, we used BCG, an attenuated mycobacterial strain less virulent than *M. tuberculosis* H37Rv, which allowed for normalization of bioactive TNF concentrations between WT and TNFRp75$^{-/-}$ BMDCs and compared WT and TNFRp75$^{-/-}$ activation after infection. If TNFRp75-mediated signaling was the mechanism of immune inhibition, we would expect decreased activation of WT versus TNFRp75$^{-/-}$ BMDCs when bioactive TNF concentrations were equal. On the contrary, WT BMDCs showed increased activation, which indicated that membrane-bound TNFRp75 may in fact supplement TNFRp55 signaling, as opposed to eliciting an inhibitory effect. We previously reported no difference in disease outcome between WT and TNFRp75$^{-/-}$ mice using BCG (33); based on our present data, this may reflect that TNFRp55 signaling is sufficient to control disease when sufficient bioactive TNF is available. To further confirm that it is soluble TNFRp75 and its ability to decrease bioactive TNF that impedes protection in WT mice, and not TNFRp75-mediated signaling, TNFRp75$^{-/-}$ BMDCs (which have neither membrane-bound nor soluble TNFRp75) were reconstituted with soluble recombinant TNFRp75. The data clearly showed a dose-dependent reduction in DC activation when soluble TNFRp75 was administered to TNFRp75$^{-/-}$ BMDCs, with IL-12p40 concentrations similar to those of WT BMDCs. This argues convincingly in favor of TNFRp75 shedding and consequent reduction in TNF bioavailability as the mechanism of immune regulation during *M. tuberculosis* infection.

Interestingly, the absence of both TNFRp55 and TNFRp75 resulted in significantly lower IL-12p40 levels than when only TNFRp55 was deleted. The small but repeatable earlier susceptibility of TNFRp55/75$^{-/-}$ versus TNFRp55$^{-/-}$ mice could therefore be due to the small discrepancy in DC activation between the strains.

In summary, our present findings demonstrated that TNFRp75$^{-/-}$ mice present with enhanced protective immunity against aerosol *M. tuberculosis* infection. Moreover, we clearly demonstrated inhibition of *M. tuberculosis*–specific Th1 immune responses by soluble TNFRp75 and identified TNF-mediated DC activation as a critical factor determining disease outcome. We have therefore identified TNFRp75 as a viable host-specific target that could potentially be exploited for therapeutic application to improve outcome of disease during *M. tuberculosis* infection.

Methods

Mice. C57BL/6 WT control, TNFRp55$^{-/-}$ (*Tnfrsf1a*$^{-/-}$; ref. 53), and TNFRp75$^{-/-}$ (*Tnfrsf1b*$^{-/-}$; ref. 54) mice were obtained from Jackson Laboratories; double-deficient TNFRp55/75$^{-/-}$ mice were generated by mating *Tnfrsf1b*$^{-/-}$ and *Tnfrsf1a*$^{-/-}$ mice. All animals were bred and housed in individually ventilated cages under specific pathogen–free conditions in the animal facility of the University of Cape Town. Male and female mice were provided food and water ad libitum and used in experiments at 8–12 weeks of age. Genotypes of the respective mouse strains were confirmed by PCR analysis of tail biopsies.

Antibodies. The following antibodies were used (all from BD Biosciences — Pharmingen): FITC-conjugated rat IgG2a (clone R35-95), PE-conjugated rat IgG2a (clone R35-95), APC-conjugated rat IgG2a (clone R4005), PE-conjugated rat IgG2b (clone R35-95), FITC-conjugated hamster IgG (clone G70-204), PE-conjugated hamster IgG (clone G70-204), PE-conjugated rat anti-mouse CD120b (clone HN102), PE-conjugated anti-mouse CD44 (Pgp-1) (clone IM7), PE-conjugated rat anti-mouse I-A/I-E (clone M5/114.15.2), PE-conjugated hamster anti-mouse CD80 (clone 16-10A1), PE-conjugated rat anti-mouse CD86 (clone GL1), PE-conjugated anti-mouse CD8a (Ly-2) (clone 53-6.7), FITC-conjugated anti-mouse CD8a (Ly-2) (clone 53-6.7), FITC-conjugated hamster anti-mouse CD11c (clone HL3), FITC-conjugated rat anti-mouse IFN-γ (clone XMG1.2), APC-conjugated rat anti-mouse CD11b (clone M1/70), APC-conjugated rat anti-mouse CD4 (clone RM4-5), rat anti-mouse CD16/CD32 (clone 2.4G2), anti-mouse CD3e (clone 145-2c11), and anti-mouse CD28 (clone 37.51).

Mycobacteria and infection. M. tuberculosis H37Rv or *M. bovis* BCG was grown in Difco Middlesbrook 7H9 medium containing 0.5% glycerol and enriched with 10% OADC. Cultures were incubated at 37°C and grown until log phase. A frozen aliquot of *M. tuberculosis* H37Rv was rapidly thawed at 37°C, passed 30 times through a 29.5-gauge needle, and diluted in sterile saline. Mice were infected using a Glas-Col Inhalation Exposure System (model A4224). The pulmonary infection dose was confirmed by sacrificing 10 mice 1 day after infection and plating the homogenized lung tissue on Difco Middlesbrook 7H10 agar plates in 10-fold serial dilutions. Plates were semi-sealed in plastic bags and then incubated for 17–21 days at 37°C, after which the number of mycobacterial colonies was counted and the infection dose calculated.

Microscopic analysis. Mice were sacrificed, and organs were fixed in phosphate-buffered formalin. Photographic images were first captured with a Nikon 4500 digital camera and analyzed using Nikon View 5 software, after which they were embedded in paraffin wax. Tissues were sectioned at 2–3 μm, stained with H&E and Ziehl-Neelsen, and mounted with Canada balsam. Images of stained tissue sections were captured using a Nikon DXM 1200 digital still camera attached to a Nikon Eclipse E400 microscope and ACT-1 software.

Bacterial burden assessment. Mice were killed at defined time points, and mycobacterial burdens in the lungs, liver, and spleen were determined by CFU enumeration. Briefly, organs were homogenized in 1–2 ml sterile saline containing 0.04% Tween 80, and tissue homogenates were plated in 10-fold serial dilution in duplicate on Difco Middlesbrook 7H10 agar (BD). Mycobacterial cultures were semi-sealed in plastic bags and incubated for 18–21 days at 37°C, after which mycobacterial colonies were counted and final organ burdens calculated.

ELISA. Cytokine and soluble receptor sample concentrations were assessed by ELISA as described by the manufacturer. Briefly, infected lungs were removed at the indicated day after infection and homogenized in 1 ml sterile saline containing 0.04% Tween 80. Homogenates were subsequently centrifuged twice at 405 *g* for 10 minutes at 4°C, and the supernatant was aliquoted and stored at –80°C for further analysis. In addition, culture supernatants from macrophages and DCs were removed, centrifuged twice at 405 *g* for 10 minutes at 4°C, and then aliquoted and stored at –80°C for further analysis. All ELISA reagents were purchased from R&D Systems, and absorbances were read at 405 nm using a VERSAmax Tunable Microplate Reader (Molecular Devices Corp.). Data were analyzed using SoftMax Pro version 4.3 software (Molecular Devices Corp.).

Bioactive TNF assay. Bioactive TNF was determined using the TNF-sensitive fibroblast cell line WEHI 164, clone 13. An aliquot of WEHI cells was thawed at 37°C and cultured in a 90-mm tissue culture petri dish (Bibby Sterilin) containing 10 ml WEHI Complete medium (RPMI supplemented with 10% FCS, 0.5× amino acid supplement, 10 U/ml penicillin, and 10 μg/ml streptomycin) until confluent. Cells were harvested in trypsin/EDTA and seeded at 2×10^4 cells/well in a 96-well tissue culture plate (Nunclon). Cells were allowed to adhere overnight by incubating at 37°C with 5% CO_2. rTNF standards (BD Biosciences — Pharmingen) were prepared in 2-fold serial dilution at a concentration range of 8–0.06 pg/ml and, together with samples, was added to WEHI cells and incubated at 37°C with 5% CO_2 for 18 hours. 50 μl of 2-mg/ml MTT (Sigma-Aldrich) was added to the samples and incubated at 37°C for 2 hours, after which the supernatant was discarded by aspiration. 50 μl WEHI detection solution (67% propanol, 0.32% HCL, and 6.7% SDS) was added to each well, and samples were read at 570 nm with reference filter at 690 nm using a VERSAmax Tunable Microplate Reader (Molecular Devices Corp.). Data were analyzed using SoftMax Pro version 4.3 software (Molecular Devices Corp.).

DC cultures and stimulation. Femurs were collected from 6- to 8-week-old mice of each strain subsequent to sacrifice by cervical dislocation. The femurs were rinsed in 70% ethanol and placed in 5 ml ice-cold complete BM-derived macrophage (BMDM) medium (RPMI supplemented with 30% L929, 20% FCS, 10 mM L-glutamine, 100 U/ml penicillin, and 100 μg/ml streptomycin) or complete DC medium (DCM) (RPMI supplemented with 50% GM-CSF conditioned medium, 10% FCS, 2 mM L-glutamine, 50 μM 20-mercaptoethanol, 100 U/ml penicillin, and 100 μg/ml streptomycin). The epiphyses of the femurs were removed with a sterile scalpel blade, and the bone was flushed with appropriate complete medium. Harvested cells were centrifuged at 405 RCF and resuspended in 1 ml complete macrophage medium for macrophage culture or 1 ml complete DCM for DC culture, counted, and seeded at 2×10^6 cells in 90-mm Sterilin bacteriological plates (Bibby Sterilin) containing 10 ml of the appropriate complete medium.

DCs were seeded at 5×10^5 cells/well in 48-well plates to obtain culture supernatants for cytokine and soluble TNFR analysis by ELISA, or at 2×10^6 cells in 90-mm culture plates (Bibby Sterilin) for analysis of activation by flow cytometry. Culture supernatants were aspirated and cells incubated with either medium alone, *M. bovis* BCG or with *M. tuberculosis* H37Rv at a MOI of 5:1 with or without anti-TNFRp75 monoclonal antibody (2 μg/ml, clone TR75-32) or rTNFRp75 (50 ng/ml or 3 μg/ml, R&D Systems). Cells were stimulated for 4 or 24 hours at 37°C with 5% CO_2. Cells were harvested and counted, and 1×10^6 cells analyzed by flow cytometry. Supernatants were collected from the 48 well plates at the indicated time points.

BAL. Mice were euthanized and dissected to reveal the trachea. An 18-gauge cannula was inserted into the trachea, and BALF was collected by doing 2 lavages each time, aspirating 10 times with 300 μl sterile PBS. The BALF was aliquoted and stored at –80°C for cytokine and TNFR analysis by ELISA. BAL cells were collected by doing 3 lavages each using 700 μl sterile PBS. Cells were kept on ice for flow cytometric analysis.

Whole-lung harvesting and tissue preparation. Mice were humanely euthanized and exsanguinated via the femoral vein. The thoracic cavity was opened to expose the heart and lungs, and the pulmonary vasculature was perfused with 5 ml PBS containing 20 U/ml heparin (Bodene [PTY] Ltd.). Lungs were removed and dissected into smaller pieces (2–3 mm) using a scalpel blade, and lung pieces were incubated with rotation for 90 minutes at 37°C in 10 ml DMEM supplemented with 50 U/ml collagenase 1 (Worthington Biomedical Corp.) and 13 U/ml DNase 1 (Boehringer Mannheim). Digested lung pieces were passed through a 70-μm cell strainer prior to centrifugation at 405 RCF at 4°C for 10 minutes. Cells were washed with complete restimulation medium (RPMI supplemented with 5% FCS, 2 mM L-glutamine, 50 μM 2-mercaptoethanol, 100 U/ml penicillin, and 100 μg/ml streptomycin), and red blood cells were lysed in 5 ml/lung red blood cell lysing buffer. Cells were left on ice for 1 minute, and 5 ml complete restimulation medium was added prior to centrifugation at 405 RCF at 4°C for 10 minutes. Cells were then either washed in 1× PBS or in complete restimulation medium, or counted for cell staining or restimulation assays. Single-cell suspensions of LNs were prepared by passage through 70-μm cell strainers prior to centrifugation at 4°C for 10 minutes. Similarly, cells were then either washed in 1× PBS or in complete restimulation medium for cell staining or restimulation.

Lung and LN restimulation. 2.2×10^6 cells/well were seeded in a 96-well round-bottomed nunc plate (Nunclon). Cells were stimulated with ESAT6 (10 μg/ml), *M. tuberculosis* at an MOI of 5:1, or anti-CD3/anti-CD28 diluted in complete restimulation medium at 37°C for a total of 6 hours with medium as a control. After the first 2 hours, Brefeldin A (Epicenter Biotechnologies) was added to a final concentration of 5 μg/ml. For anti-CD3/anti-CD28 restimulation, wells were coated overnight with anti-CD3/anti-CD28 (5 μg/ml in a volume of 50 μl), and the antibody cocktail was aspirated off prior to the addition of cells. After 6 hours of stimulation, cells were centrifuged for 5 minutes at 514 RCF, resuspended in 220 μl FACS buffer, and replated into 96-well v-bottomed sterilin plates (Bibby Sterilin) for analysis by flow cytometry.

Flow cytometry. BMDMs, BMDCs, or single-cell suspensions of lungs or LNs were labeled in 96-well plates (Bibby Sterilin) with the indicated antibodies. Samples were analyzed on a FACS Calibur (BD) flow cytometer using Cell Quest software (BD). Briefly, 1×10^6 BMDMs or BMDCs and 2×10^6 lung cells or LN cells were stained with the required antibodies or IgG control antibodies. For intracellular staining, saponin buffer was used to permeabilize the cells. All cells were fixed overnight in 2% paraformaldehyde before analysis.

RNA isolation. Total RNA was isolated from cultured DCs at 4 and 24 hours after *M. tuberculosis* infection using TriReagent and purified using the RNeasy RNA Extraction kit (Quiagen) according to the manufacturer's instructions.

Quantitative RT-PCR. cDNA synthesis was performed using the Transcriptor First Strand cDNA Synthesis Kit (Roche), and RT-PCR was performed using the Roche LightCycler 480 SYBR Green 1 Kit (Roche) according to the manufacturer's instructions. The following primers were used: *Tnf* forward, 5′-TCTCATCAGTTCTATGGCCC-3′; *Tnf* reverse, 5′-GGGAGTAGACAAGGTACAAC-3′; ribosomal S12 (*rS12*) for-

ward, 5′-GGAAGGCATAGCTGCTGGAGGT-3′; *rS12* reverse, 5′-CGATGACATCCTTGGCCTGA-3′. Relative *Tnf* mRNA expression was calculated by dividing the *Tnf* value by the *rS12* (housekeeping gene) value.

Statistics. Data are expressed as mean ± SEM. Statistical analysis was performed by ANOVA using GraphPad Prism software (version 4.01). For mortality studies, analysis was performed using the log-rank test. A *P* value less than 0.05 was considered significant.

Study approval. The Research Ethics Committee of the University of Cape Town approved all experiments.

Acknowledgments

This study was supported by the National Research Foundation (South Africa), the Medical Research Council (South Africa), University of Cape Town, National Health and Laboratory Services (South Africa), and the European Union (FP6 NEST project no. 028190 "TB REACT"). Research was carried out within the scope of the Franco/South African Laboratory "TB Immunity" (Associated International Laboratory [AIL] no. 236). The authors thank Marylin Tyler for contributing to the histopathology, Natalie Neuwenhuizen for constructive critique of the manuscript, and the staff of the Division of Immunology and the Animal Unit at UCT for contributing to animal care and technical support.

Received for publication October 22, 2013, and accepted in revised form December 19, 2013.

Address correspondence to: Muazzam Jacobs, Room S1.33, Level 1, Werner Beit South, Institute of Infectious Disease and Molecular Medicine, Division of Immunology, Health Sciences Faculty, University of Cape Town, Anzio Road 7925 Observatory, Cape Town, South Africa. Phone: 27.21.406.6078; Fax: 27.21.406.6078; E-mail: Muazzam.Jacobs@uct.ac.za.

1. Locksley RM, Killeen N, Lenardo MJ. The TNF and TNF receptor superfamilies: integrating mammalian biology. *Cell*. 2001;104(4):487–501.
2. Schluter D, Deckert M. The divergent role of tumor necrosis factor receptors in infectious diseases. *Microbes Infect*. 2000;2(10):1285–1292.
3. Perez C, Albert I, DeFay K, Zachariades N, Gooding L, Kriegler M. A nonsecretable cell surface mutant of tumor necrosis factor (TNF) kills by cell-to-cell contact. *Cell*. 1990;63(2):251–258.
4. Orlinick JR, Chao MV. TNF-related ligands and their receptors. *Cell Signal*. 1998;10(8):543–551.
5. Wajant H, Scheurich P. Tumor necrosis factor receptor-associated factor (TRAF) 2 and its role in TNF signaling. *Int J Biochem Cell Biol*. 2001;33(1):19–32.
6. Corti A, et al. Upregulation of p75 tumor necrosis factor α receptor in Mycobacterium avium-infected mice: evidence for a functional role. *Infect Immun*. 1999;67(11):5762–5767.
7. Balcewicz-Sablinska MK, Keane J, Kornfeld H, Remold HG. Pathogenic Mycobacterium tuberculosis evades apoptosis of host macrophages by release of TNF-R2, resulting in inactivation of TNF-α. *J Immunol*. 1998;161(5):2636–2641.
8. Aderka D, Engelmann H, Maor Y, Brakebusch C, Wallach D. Stabilization of the bioactivity of tumor necrosis factor by its soluble receptors. *J Exp Med*. 1992;175(2):323–329.
9. Roach DR, Bean AG, Demangel C, France MP, Briscoe H, Britton WJ. TNF regulates chemokine induction essential for cell recruitment, granuloma formation, and clearance of mycobacterial infection. *J Immunol*. 2002;168(9):4620–4627.
10. Kaneko H, et al. Role of tumor necrosis factor-alpha in Mycobacterium-induced granuloma formation in tumor necrosis factor-α-deficient mice. *Lab Invest*. 1999;79(4):379–386.
11. Kindler V, Sappino AP, Grau GE, Piguet PF, Vassalli P. The inducing role of tumor necrosis factor in the development of bactericidal granulomas during BCG infection. *Cell*. 1989;56(5):731–740.
12. Eriks IS, Emerson CL. Temporal effect of tumor necrosis factor alpha on murine macrophages infected with Mycobacterium avium. *Infect Immun*. 1997;65(6):2100–2106.
13. Bean AG, et al. Structural deficiencies in granuloma formation in TNF gene-targeted mice underlie the heightened susceptibility to aerosol Mycobacterium tuberculosis infection, which is not compensated for by lymphotoxin. *J Immunol*. 1999;162(6):3504–3511.
14. Zganiacz A, et al. TNF-α is a critical negative regulator of type 1 immune activation during intracellular bacterial infection. *J Clin Invest*. 2004; 113(3):401–413.
15. Jacobs M, et al. Reactivation of tuberculosis by tumor necrosis factor neutralization. *Eur Cytokine Netw*. 2007;18(1):5–13.
16. Jacobs M, et al. Tumor necrosis factor is critical to control tuberculosis infection. *Microbes Infect*. 2007;9(5):623–628.
17. Fremond C, et al. Membrane TNF confers protection to acute mycobacterial infection. *Respir Res*. 2005;6:136.
18. Olleros ML, et al. Transmembrane TNF induces an efficient cell-mediated immunity and resistance to Mycobacterium bovis bacillus Calmette-Guerin infection in the absence of secreted TNF and lymphotoxin-α. *J Immunol*. 2002;168(7):3394–3401.
19. Olleros ML, et al. Contribution of transmembrane tumor necrosis factor to host defense against Mycobacterium bovis bacillus Calmette-guerin and Mycobacterium tuberculosis infections. *Am J Pathol*. 2005;166(4):1109–1120.
20. Probert L, et al. Dissection of the pathologies induced by transmembrane and wild-type tumor necrosis factor in transgenic mice. *J Leukoc Biol*. 1996;59(4):518–525.
21. Saunders BM, Tran S, Ruuls S, Sedgwick JD, Briscoe H, Britton WJ. Transmembrane TNF is sufficient to initiate cell migration and granuloma formation and provide acute, but not long-term, control of Mycobacterium tuberculosis infection. *J Immunol*. 2005;174(8):4852–4859.
22. Allie N, et al. Protective role of membrane tumour necrosis factor in the host's resistance to mycobacterial infection. *Immunology*. 2008;125(4):522–534.
23. Dambuza I, et al. Efficacy of membrane TNF mediated host resistance is dependent on mycobacterial virulence. *Tuberculosis (Edinb)*. 2008;88(3):221–234.
24. Flynn JL, et al. Tumor necrosis factor-α is required in the protective immune response against Mycobacterium tuberculosis in mice. *Immunity*. 1995;2(6):561–572.
25. Jacobs M, et al. Correction of defective host response to Mycobacterium bovis BCG infection in TNF-deficient mice by bone marrow transplantation. *Lab Invest*. 2000;80(6):901–914.
26. Senaldi G, Yin S, Shaklee CL, Piguet PF, Mak TW, Ulich TR. Corynebacterium parvum- and Mycobacterium bovis bacillus Calmette-Guerin-induced granuloma formation is inhibited in TNF receptor I (TNF-RI) knockout mice and by treatment with soluble TNF-RI. *J Immunol*. 1996;157(11):5022–5026.
27. Garcia I, et al. Lethal Mycobacterium bovis Bacillus Calmette Guerin infection in nitric oxide synthase 2-deficient mice: cell-mediated immunity requires nitric oxide synthase 2. *Lab Invest*. 2000;80(9):1385–1397.
28. Moreira AL, Wang J, Sarno EN, Kaplan G. Thalidomide protects mice against LPS-induced shock. *Braz J Med Biol Res*. 1997;30(10):1199–1207.
29. Engele M, et al. Induction of TNF in human alveolar macrophages as a potential evasion mechanism of virulent Mycobacterium tuberculosis. *J Immunol*. 2002;168(3):1328–1337.
30. Ehlers S, Kutsch S, Ehlers EM, Benini J, Pfeffer K. Lethal granuloma disintegration in mycobacteria-infected TNFRp55$^{-/-}$ mice is dependent on T cells and IL-12. *J Immunol*. 2000;165(1):483–492.
31. Flynn JL, Goldstein MM, Triebold KJ, Sypek J, Wolf S, Bloom BR. IL-12 increases resistance of BALB/c mice to Mycobacterium tuberculosis infection. *J Immunol*. 1995;155(5):2515–2524.
32. Peschon JJ, et al. TNF receptor-deficient mice reveal divergent roles for p55 and p75 in several models of inflammation. *J Immunol*. 1998;160(2):943–952.
33. Jacobs M, Brown N, Allie N, Chetty K, Ryffel B. Tumor necrosis factor receptor 2 plays a minor role for mycobacterial immunity. *Pathobiology*. 2000;68(2):68–75.
34. Lucas R, et al. Crucial role of tumor necrosis factor (TNF) receptor 2 and membrane-bound TNF in experimental cerebral malaria. *Eur J Immunol*. 1997;27(7):1719–1725.
35. Khader SA, et al. Interleukin 12p40 is required for dendritic cell migration and T cell priming after Mycobacterium tuberculosis infection. *J Exp Med*. 2006;203(7):1805–1815.
36. Redford PS, Murray PJ, O'Garra A. The role of IL-10 in immune regulation during *M. tuberculosis* infection. *Mucosal Immunol*. 2011;4(3):261–270.
37. Wynn TA. IL-13 effector functions. *Annu Rev Immunol*. 2003;21:425–456.
38. De Smedt T, Van Mechelen M, De Becker G, Urbain J, Leo O, Moser M. Effect of interleukin-10 on dendritic cell maturation and function. *Eur J Immunol*. 1997;27(5):1229–1235.
39. Webb DC, Cai Y, Matthaei KI, Foster PS. Comparative roles of IL-4, IL-13, and IL-4Rα in dendritic cell maturation and CD4+ Th2 cell function. *J Immunol*. 2007;178(1):219–227.
40. Islam N, et al. Role of cellular activation and tumor necrosis factor-α in the early expression of Mycobacterium tuberculosis 85B mRNA in human alveolar macrophages. *J Infect Dis*. 2004; 190(2):341–351.
41. Kim EY, Teh HS. TNF type 2 receptor (p75) lowers the threshold of T cell activation. *J Immunol*. 2001;167(12):6812–6820.
42. MacEwan DJ. TNF receptor subtype signalling: differences and cellular consequences. *Cell Signal*. 2002;14(6):477–492.
43. Reis e Sousa C, Stahl PD, Austyn JM. Phagocytosis of antigens by Langerhans cells in vitro. *J Exp Med*. 1993;178(2):509–519.
44. Bottomly K. T cells and dendritic cells get intimate. *Science*. 1999;283(5405):1124–1125.

45. Wolf AJ, et al. Initiation of the adaptive immune response to Mycobacterium tuberculosis depends on antigen production in the local lymph node, not the lungs. *J Exp Med*. 2008;205(1):105–115.
46. Bodnar KA, Serbina NV, Flynn JL. Fate of Mycobacterium tuberculosis within murine dendritic cells. *Infect Immun*. 2001;69(2):800–809.
47. Serbina NV, Salazar-Mather TP, Biron CA, Kuziel WA, Pamer EG. TNF/iNOS-producing dendritic cells mediate innate immune defense against bacterial infection. *Immunity*. 2003;19(1):59–70.
48. Cooper AM, Magram J, Ferrante J, Orme IM. Interleukin 12 (IL-12) is crucial to the development of protective immunity in mice intravenously infected with mycobacterium tuberculosis. *J Exp Med*. 1997;186(1):39–45.
49. de Jong R, Janson AA, Faber WR, Naafs B, Ottenhoff TH. IL-2 and IL-12 act in synergy to overcome antigen-specific T cell unresponsiveness in mycobacterial disease. *J Immunol*. 1997;159(2):786–793.
50. Flynn JL, Chan J. Immunology of tuberculosis. *Annu Rev Immunol*. 2001;19:93–129.
51. Marino S, Pawar S, Fuller CL, Reinhart TA, Flynn JL, Kirschner DE. Dendritic cell trafficking and antigen presentation in the human immune response to Mycobacterium tuberculosis. *J Immunol*. 2004;173(1):494–506.
52. Flesch IE, Kaufmann SH. Activation of tuberculostatic macrophage functions by gamma interferon, interleukin-4, and tumor necrosis factor. *Infect Immun*. 1990;58(8):2675–2677.
53. Pfeffer K, et al. Mice deficient for the 55 kd tumor necrosis factor receptor are resistant to endotoxic shock, yet succumb to L. monocytogenes infection. *Cell*. 1993;73(3):457–467.
54. Erickson SL, et al. Decreased sensitivity to tumour-necrosis factor but normal T-cell development in TNF receptor-2-deficient mice. *Nature*. 1994;372(6506):560–563.